

## Excited state properties and acid–base equilibria of *trans*-2-styrylbenzoxazoles

Tarek A. Fayed\*, Safaa El-Din H. Etaiw, Hayam M. Khatab

Department of Chemistry, Faculty of Science, Tanta University, 31527-Tanta, Egypt

Received 16 June 2004; received in revised form 1 August 2004; accepted 9 August 2004

Available online 12 September 2004

### Abstract

The photophysics of some styryl dyes namely; 2-(4'-*R*-styryl)benzoxazole, (*R*-SBO where *R* = NMe<sub>2</sub>, 2',4'-OCH<sub>3</sub>, OCH<sub>3</sub>, CH<sub>3</sub>, H, Cl and CN) were investigated in several organic solvents by using steady-state absorption and emission as well as frequency modulation spectroscopic techniques. The absorption and fluorescence characteristics (such as fluorescence maximum, quantum yield and lifetime) are tuned by substitution, solvent and protonation. Depending on the substituent, the benzoxazole ring can be an electron donor (as in the case of CN-SBO) or an electron acceptor (as in the other derivatives). All of the solid derivatives exhibit intense emission with colours changing from blue to green and yellow, depending on the substituent. The protonation constants of the benzoxazole nitrogen atom, in both the ground and excited state, were also determined. The obtained values are strongly substituent dependent, and indicate that the basicity of all derivatives (except for CN-SBO) increases upon excitation. In addition, the *trans* → *cis* photoisomerization quantum yields were determined in some solvents. The values depend on the nature of the substituent and the solvent characteristics like the polarity and viscosity. The effects of solvent polarity and viscosity as well as the substituent on both the fluorescence and isomerization quantum yields, suggested that the two-deactivation pathways are competitive. The role of the intramolecular charge transfer interaction in controlling the properties of the ground and excited state of the present styryl dyes is also discussed.

© 2004 Elsevier B.V. All rights reserved.

**Keywords:** Styrylbenzoxazole; Fluorescence; Photoisomerization; Protonation; Charge transfer; Solid emission.

### 1. Introduction

The excited state properties of 1,2-diarylethylenes, whose prototype is stilbene, have been extensively studied by both theoretical and experimental approaches [1–5]. Most interest lies in their role as simple models for conformational properties and *trans*–*cis* photoisomerization reactions around ethylenic double bonds in biological systems [6]. Practical attention has been given to study the photophysics and photoisomerization of diarylethylenes containing hetero-atoms specially the aza-analogues of stilbene [7–10]. These studies have pointed out that the *n*– $\pi^*$ -states introduced by the pyridinic nitrogen hetero-atom are playing an important role

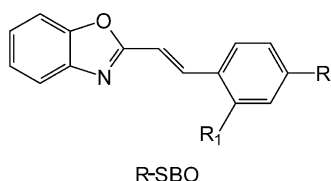
in perturbing the radiative and the reactive *trans*–*cis* photoisomerization deactivation pathways of the lowest excited singlet state, compared to the parent hydrocarbon (*trans*-stilbene).

Styrylbenzoxazoles and their benzothiazole derivatives, specially their Pt(II) complexes, have shown biological activity as cytotoxic [11,12]. Also, styrylbenzoxazoles are used as gastric acid secretion inhibitors [13]. In addition, they are used in photoconductors [14]. Furthermore, condensation polymers containing styrylbenzoxazoles are useful for manufacturing of drink and food containers resistant to heat and light [15]. Despite of these important applications, few is reported about the photophysics and photochemistry of this class of diarylethylenes [16–21].

Therefore, the present study deals with studying the photophysical properties, *trans*–*cis* photoisomerization and the acid–base equilibria of several *trans* 2-(4'-*R*-styryl)-

\* Corresponding author. Tel.: +20 40 3120708; fax: +20 40 3350804.

E-mail addresses: [tfayed2003@yahoo.co.uk](mailto:tfayed2003@yahoo.co.uk) (T.A. Fayed), [safaahe@gega.net](mailto:safaahe@gega.net) (S. H. Etaiw).



Scheme 1.  $R = -\text{NMe}_2$ ,  $-\text{OCH}_3$ ,  $-\text{CH}_3$ ,  $-\text{H}$ ,  $-\text{Cl}$ , and  $-\text{CN}$ ;  $R = R_1 = -\text{OCH}_3$ .

benzoxazoles, *R*-SBO [ $R = \text{NMe}_2$ , 2',4'- $\text{OCH}_3$ ,  $\text{OCH}_3$ ,  $\text{CH}_3$ ,  $\text{H}$ ,  $\text{Cl}$  and  $\text{CN}$ ], Scheme 1, which were synthesized for this purpose. An interesting behaviour of this family, is the modulation of their ground and excited state properties by substitution, environment and protonation. These features may render them as suitable candidates for the construction of light emitting devices necessary for optoelectronic applications.

## 2. Experimental

The styrylbenzoxazoles under investigation were prepared by condensation of 2-methylbenzoxazole with substituted benzaldehyde as reported previously [19]. The products were crystallized twice from dry ethanol and characterized by TLC, elemental analysis, IR and UV–vis spectral measurements.

Spectroscopic grade solvents (from Aldrich or BDH) were used as received. All solvents were non-fluorescent in the region of fluorescence measurements. Double distilled water was used for preparation of buffer solutions. Analytical grade orthophosphoric acid and NaOH were used as received.

Aqueous buffer solutions were prepared by mixing appropriate volumes of NaOH and  $\text{H}_3\text{PO}_4$ , 0.1 M each. Solutions having  $\text{pH} < 2$  were prepared following Hammett's acidity ( $H_0$ ) scale [22].

Steady-state absorption and emission measurements were carried out using a Shimadzu UV-3101PC scanning spectrophotometer and a Perkin-Elmer LS 50B spectrofluorometer, respectively. The fluorescence of solid crystals was recorded by using a special holder for solid samples, where the emission intensity was measured from the surface at right angle to the excitation source. Continuous irradiation was carried out by using the Xe-lamp of the fluorometer. By this method the wavelength and the intensity of the excitation light could be controlled easily. The intensity of the irradiation light was measured by application of ferrioxalate actinometry [23]. The fluorescence quantum yields ( $\phi_f$ ) were measured relative to quinine sulphate in 0.1 N  $\text{H}_2\text{SO}_4$  as a standard ( $\phi_f = 0.54$ ) [24]. The samples were excited around their absorption maximum. For determination of the *trans*  $\rightarrow$  *cis* photoisomerization quantum yields ( $\phi_t$ ), the method described by Gauglitz [25] was used. The fluorescence lifetime was measured by using LED-modulation spectroscopy with ultrabright light emitting diodes ( $\lambda_{\text{max}} = 390 \text{ nm}$  and 14 nm

FWHM at 120 MHz modulation frequency) as described previously [26]. All measurements were carried out under red light at  $25^\circ\text{C} \pm 1$  using fresh solutions ( $2 \times 10^{-5} \text{ M}$ ).

## 3. Results and discussion

### 3.1. Absorption and fluorescence spectra

The absorption and fluorescence spectra of some selected *trans*-*R*-SBO recorded in ethanol are shown in Fig. 1, while the spectral data are collected in Table 1. The longest wavelength absorption and emission bands are strongly influenced by the substituent at the 4'-position of the phenyl ring. Both the absorption and emission maxima of the parent SBO are shifted from 322 and 386 nm to 394 and 482 nm, respectively, on introducing of a strong electron donating substituent as in the case of  $\text{Me}_2\text{N}$ -SBO. Also, the spectra exhibit a pronounced structure on going from strong electron donating substituents to less or electron withdrawing ones. In addition, the absorption bands are characterized by high molar absorp-

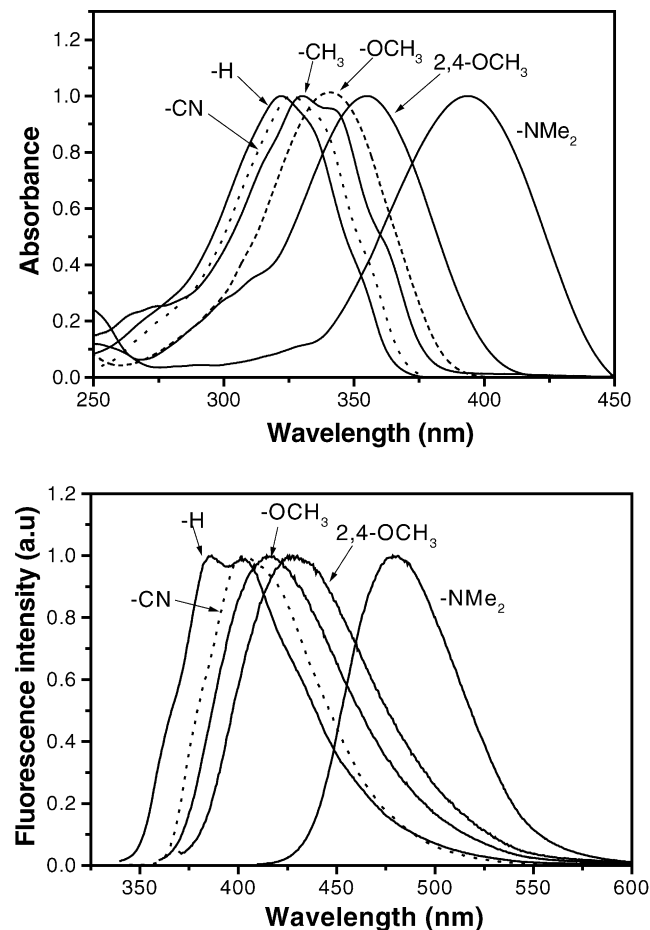


Fig. 1. Electronic absorption and fluorescence spectra of selected, styrylbenzoxazoles recorded in ethanol (upper and lower panel, respectively). The substituents are shown in the figure.

Table 1

Spectral data for *R*-SBO in ethanol and solid crystals, the Hammett substituent constants ( $\sigma_p^+$ ) and the ionization potentials (I.P.) of the substituted phenyl group

<i>R</i>	$\sigma_p^+$	I.P. (eV)	$\lambda_{\max}^a$ (nm)	$\epsilon_{\max}$ (l mol <sup>-1</sup> cm <sup>-1</sup> )	$\lambda_{\max}^f$ (nm)	$E_{0,0}$ (kcal mol <sup>-1</sup> )	$\lambda_{\max}^f$ (nm) <sup>a</sup>
NMe <sub>2</sub>	-1.7	7.12	394	41000	482	65.12	533(+)
2',4'-OCH <sub>3</sub>	—	—	355	35875	431	73.31	480(+)
OCH <sub>3</sub>	-0.78	8.21	341	50650	417	75.63	465(+)
CH <sub>3</sub>	-0.31	8.82	328	52300	418	77.9	500(+)
H	0.0	9.24	322	54500	386	80.08	425(+)
Cl	0.11	9.07	326	51282	391	79.19	440
CN	0.66	9.62	329	40222	403	77.06	473

<sup>a</sup> Fluorescence maximum of solid crystals, (+); highly fluorescent.

tivities indicating a strongly allowed  $\pi$ - $\pi^*$  transition. The large bathochromic shift of the spectral maxima with increasing the electron donor strength of the substituent is consistent with a charge transfer (CT) character of the corresponding electronic transition. These results indicate a sizeable electronic interaction between the substituted phenyl ring, as an electron donor, and the benzoxazole ring, as an electron acceptor, via the intervening double bond. This conclusion is supported by Fig. 2 which illustrates that the order affecting the energy of the 0,0-transition ( $E_{0,0}$ ) of the styrylbenzoxazoles is related to the ionization energy of the substituted phenyl ring. The wavelengths of the 0,0-transitions were estimated from the intersection of the normalized absorption and fluorescence spectra. The much lower  $E_{0,0}$ -value of Me<sub>2</sub>N-SBO is due to participation of the nitrogen lone-pair in the conjugation along the whole molecule [27]. Also, according to Fig. 2 and the data in Table 1, CN-SBO shows a lower  $E_{0,0}$ -value and red-shifted absorption and emission bands relative to the parent SBO. This order suggests an inversion in the CT direction, where the cyano-phenyl group (with greater electron attracting ability) acts as the acceptor and the benzoxazole ring acts as the donor. Confirmation of this conclusion comes from the results that the nitrogen atom of the benzoxazole ring of CN-SBO can be protonated only in strongly acidic media (vide infra).

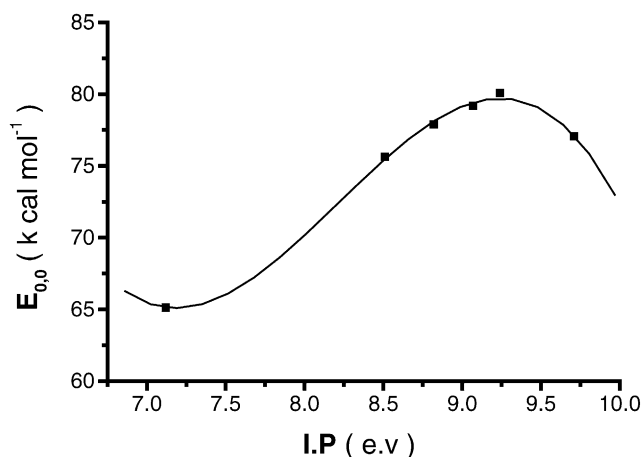


Fig. 2. Variation of the  $E_{0,0}$  energy with the ionization potential of the substituted phenyl group.

The absorption and emission spectra of *R*-SBO were also examined in various solvents having different polarities. Fig. 3 displays the spectra of CN-SBO, CH<sub>3</sub>O-SBO and Me<sub>2</sub>N-SBO in *c*-hexane and CH<sub>3</sub>CN as illustrative examples, while Table 2 collects the corresponding spectral maxima. The effects of solvent polarity on the CT absorption and emission bands of *R*-SBO, depend strongly on the nature of substituents. The spectra of H-SBO, Cl-SBO and CN-SBO reveal virtually little dependence on the solvent polarity. In contrast, styrylbenzoxazoles having electron donating substituents (Me<sub>2</sub>N, 2',4'-OCH<sub>3</sub>, OCH<sub>3</sub> and CH<sub>3</sub>) exhibit red shifts in their spectral maxima with increasing the solvent polarity. However, the shifts are more pronounced in the fluorescence spectra than in the absorption spectra. In addition to the red shift, an increase of the vibronic structure can be easily observed on going from the more polar solvents like CH<sub>3</sub>CN to the non-polar *c*-hexane. In fact, the most remarkable red shifts were observed in the case of Me<sub>2</sub>N-SBO. It is worth mentioned that the photophysics of Me<sub>2</sub>N-SBO have been investigated earlier [19,21] but it would be reconsidered to highlight the effect of substituents. The solvatochromic effect on the emission spectra of the methoxy derivatives is also ob-

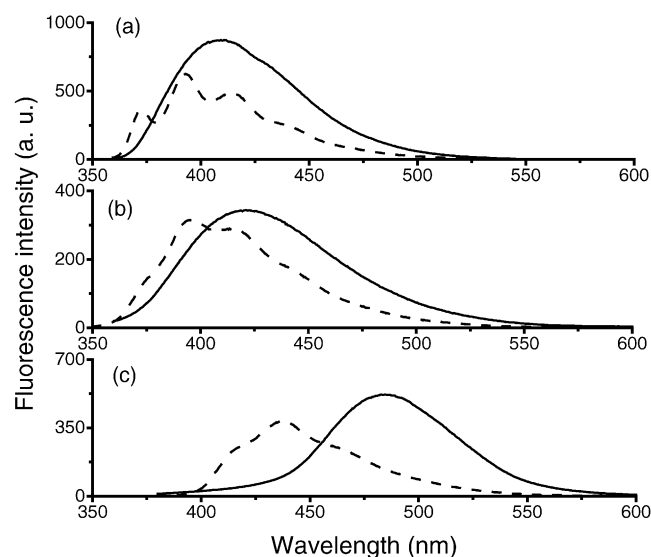


Fig. 3. Fluorescence spectra of CN-SBO (a), CH<sub>3</sub>O-SBO (b) and NMe<sub>2</sub>-SBO (c) measured in *c*-hexane (---) and CH<sub>3</sub>CN (—).

Table 2

Absorption and fluorescence maxima ( $\lambda^a$  and  $\lambda^f$  in nm, respectively) of styrylbenzoxazoles measured in different solvents

R	c-Hexane	Et-acetate	CH <sub>3</sub> CN	MeOH	DMSO
NMe <sub>2</sub> , $\lambda^a$	378	385	388	394	398
$\lambda^f$	416,438,463	464	485	488	493
2',4'-OCH <sub>3</sub> , $\lambda^a$	348	350	351	355	356
$\lambda^f$	395,416,440	423	426	431	436
OCH <sub>3</sub> , $\lambda^a$	334	337	337	341	344
$\lambda^f$	376,395,417	410	424	417	427
CH <sub>3</sub> , $\lambda^a$	325	326	326	328	331
$\lambda^f$	366,385,410	366,385	390,417	390,418	385,425
H, $\lambda^a$	321	–	321	322	–
$\lambda^f$	361,380,399	–	385,402	386,403	–
Cl, $\lambda^a$	326	–	325	326	–
$\lambda^f$	365,386,415	–	389,407	391,410	–
CN, $\lambda^a$	331	–	329	329	–
$\lambda^f$	373,393,415	–	410	403	–

served. The large bathochromic shifts of the emission bands with increasing the solvent polarity indicate greater stabilization of the excited singlet state in polar solvents. This trend is characteristic for molecules that are likely to have enlarged dipoles and CT characters in their excited singlet states [28].

Another property listed in Table 1, is the intense photoluminescence exhibited by most of the solid styrylbenzoxazoles when excited at 365 nm. This property is surprising since solutions of all compounds (except for CN-SBO) are weakly fluorescent. For many fluorophores the opposite behaviour is the typical, that is to say, despite of intense fluorescence is obtained in solutions, radiationless deactivation predominates in the crystalline state. These properties are influenced considerably by the packing effects [29], which have a decisive influence on the relaxation pathways of the excitation energy. In fact, all the investigated styrylbenzoxazoles, whose colours change noticeably with substituents, are nicely crystalline (except for CN-SBO) and shine intensively upon irradiation. The colour of the emitted radiation changes greatly with the substituent as can be seen from the shift of the emission maximum, Fig. 4. For example, the solid H-SBO

emits blue whereas the emission of the solid Me<sub>2</sub>N-SBO is yellow. Solid state photoluminescent substances are very interesting for several high-technology applications such as the fabrication of light emitting diodes [30,31].

### 3.2. Fluorescence quantum yield and lifetime

The fluorescence quantum yields ( $\phi_f$ ) of the trans-*R*-SBO, at ambient temperature, are dependent on the nature of substituent and solvent polarity, Table 3. Firstly, the fluorescence of styrylbenzoxazoles carrying electron donating groups (NMe<sub>2</sub>, 2',4'-OCH<sub>3</sub>, OCH<sub>3</sub> and CH<sub>3</sub>) in solutions, is weak, and their  $\phi_f$  is less sensitive to the solvent polarity but enhances largely with increasing the solvent viscosity. The  $\phi_f$  increases by 13–56 orders of magnitude when the solvent is changed from methanol to the highly viscous glycerol. Secondly, for H-SBO and Cl-SBO, the  $\phi_f$  is moderate and decreases significantly with increasing the polarity and hydrogen bonding ability of the solvent. A typical effect is seven folds lowering in the  $\phi_f$  of Cl-SBO in the strongly polar methanol than in *c*-hexane. An increase of the  $\phi_f$  in viscous solvents (although not large) is also observed for both styrylbenzoxazoles.

Thirdly, CN-SBO exhibits the highest fluorescence quantum yield indicating that introducing of a strong electron-withdrawing group at the 4'-position enhances strongly the

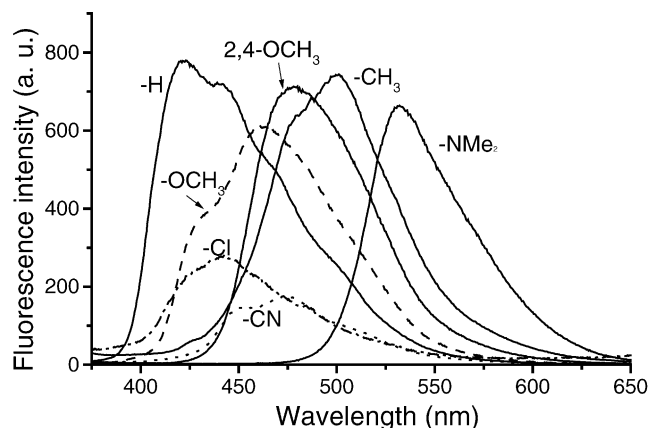


Fig. 4. Fluorescence spectra of solid crystals from *R*-SBO measured under the same conditions.

Table 3

Fluorescence quantum yields of *R*-SBO measured in different solvents at 25 °C

R	c-Hexane	CH <sub>3</sub> CN	EtOH	MeOH	Et-glycol	Glycerol
NMe <sub>2</sub>	0.006	0.006	0.005	0.004	0.017	0.141
2',4'-OCH <sub>3</sub>	0.004	0.006	0.001	0.001	0.006	0.056
OCH <sub>3</sub>	0.004	0.002	0.001	0.001	0.004	0.013
CH <sub>3</sub>	0.013	0.007	0.005	0.005	0.016	0.068
H	0.013	0.067	0.034	0.029	0.022	0.095
Cl	0.073	0.011	0.008	0.005	0.022	0.107
CN	0.751	0.524	0.389	0.361	0.409	0.481

EtOH; ethanol, MeOH; methanol, Et-glycol; ethylene glycol.

Table 4

Fluorescence lifetime ( $\tau_f$ , ns), radiative ( $k_r \times 10^8$ , s<sup>-1</sup>) and non-radiative ( $k_{nr} \times 10^8$ , s<sup>-1</sup>) rate constants for some *R*-SBO measured in some solvents

Solvent	CN-SBO			Cl-SBO			CH <sub>3</sub> -SBO		
	$\tau_f$	$k_r$	$k_{nr}$	$\tau_f$	$k_r$	$k_{nr}$	$\tau_f$	$k_r$	$k_{nr}$
<i>c</i> -Hexane	0.9	8.4	2.8	0.14	5.2	66.2	1.0	1.3	9.9
CH <sub>3</sub> CN	1.12	4.3	3.9	0.07	1.6	141.2	0.77	0.09	12.9
MeOH	0.84	4.3	7.6	<0.05	–	–	0.25	0.20	39.8
Et-glycol	1.22	3.4	4.8	–	–	–	0.74	0.23	13.3

radiative deactivation pathway of the excited singlet state in such styrylbenzoxazoles. The  $\phi_f$  of CN-SBO in *c*-hexane is 57 and 125 magnitudes higher than those of H-SBO and Me<sub>2</sub>N-SBO, respectively. Also, the  $\phi_f$  of CN-SBO decreases steadily with increasing the solvent polarity and hydrogen bonding ability, but essentially is less sensitive to the solvent viscosity. Generally, the solvent dependence of  $\phi_f$  in all *R*-SBO was not easily correlated with the properties of the medium, in particular its polarity, hydrogen bonding ability and viscosity.

The higher  $\phi_f$  of all styrylbenzoxazoles in viscous media is due to increasing of frictional forces and decreasing of the solvent free-volume necessary for the rotation-dependent non-radiative *trans*–*cis* photoisomerization process.

The lower fluorescence quantum yields characteristic for styrylbenzoxazoles carrying electron donating substituents can be attributed, at least in part, to the photoinduced intramolecular CT interaction which contributes effectively to fluorescence quenching.

Additional fluorescence parameters such as lifetime ( $\tau_f$ ), radiative ( $k_r$ ) and non-radiative ( $k_{nr}$ ) rate constants for CN-SBO, Cl-SBO and CH<sub>3</sub>-SBO are presented in Table 4. For the other derivatives, the fluorescence lifetime is shorter than 50 ps (the resolution limit of the used technique).

The rate constants of the radiative and nonradiative processes of the excited singlet state were calculated according to the relations [32];

$$k_r = \frac{\phi_f}{\tau_f} \quad \text{and} \quad k_{nr} = \frac{1 - \phi_f}{\tau_f} \quad (1)$$

The non-radiative rate includes contribution of the excited singlet state to the photoisomerization process, the singlet-triplet intersystem crossing and the internal conversion. Parallel with the  $\phi_f$  values, the  $\tau_f$  of CN-SBO in the used solvents, is longer compared to those of Cl-SBO and CH<sub>3</sub>-SBO. Due to competition between the radiative and radiationless processes,  $k_{nr}$  increases on going from CN-SBO to Cl-SBO and CH<sub>3</sub>-SBO. In non-polar solvents as cyclohexane, the fluorescence lifetime and the radiative rate are higher than the corresponding values in highly polar protic solvents like methanol. In contrast, the non-radiative decay rate increases in the same direction. However, in the rather viscous ethylene glycol, both the  $\tau_f$  and  $k_r$  are higher, which agrees well with the higher  $\phi_f$  values.

The foregoing results indicate clearly that combination of a substituted phenyl ring with a benzoxazole moiety

through an ethylenic bridge provides a unique family of tunable intrinsic fluorophores. For such a family, changes in the electronic polarization (due to introduction of different substitution groups), solvation and rotation free volumes are translated into dramatic changes in their spectral behaviour and the fluorescence characteristics. Highly emissive tunable chromophores are rare [33] although they have been attracting considerable interest as compounds for fluorescent sensors and switches [34].

### 3.3. Acid–base equilibria of substituted styrylbenzoxazoles

To correlate the protonation constants of the benzoxazole nitrogen atom with molecular structure, the absorption and fluorescence spectra of all styrylbenzoxazoles were studied in buffer solutions having different pH/*H*<sub>0</sub>-values (in the range from 5.0 to –1.17). In all cases, the absorption spectra display changes characteristic for the acid–base equilibrium with increasing the acidity of the medium. Also, the absorption and fluorescence spectra are red shifted in acidic media, Table 5. These shifts are due to mesomeric stabilization of the formed cation via the substituent group. The magnitude of these bathochromic shifts, increases strongly with increasing the electron donating ability of the substituent. For example, the absorption and emission maxima of CN-SBO are red shifted by 13 and 15 nm, respectively, while those of Me<sub>2</sub>N-SBO, are shifted by 84 and 30 nm, respectively.

The ground state protonation constants (p*K*) were calculated from the pH/*H*<sub>0</sub>-dependent absorption spectra, whereas the excited state protonation constants (p*K*<sup>\*</sup>) were calculated using Forster cycle [35]. The obtained values are listed in Table 5. It could be recognized that the p*K* value can be

Table 5

Absorption and fluorescence maxima of the neutral and protonated *R*-SBO as well as their ground and excited states protonation constants

<i>R</i>	Neutral		Protonated		p <i>K</i> <sub>a</sub>	p <i>K</i> <sub>a</sub> <sup>*</sup>
	$\lambda^a$	$\lambda^f$	$\lambda^a$	$\lambda^f$		
NMe <sub>2</sub>	388	512	472	542	3.12	10.13
2',4'-OCH <sub>3</sub>	354	475	398	485	1.35	6.73
OCH <sub>3</sub>	339	451	378	472	1.3	5.41
CH <sub>3</sub>	330	455	359	467	0.55	4.32
H	323	410	347	432	0.29	2.09
Cl	328	414	353	439	0.11	1.67
CN	334	415	347	430	–0.098	–0.66



modulated by introducing of either electron donating or electron withdrawing substituents. This was represented by the nice correlation between the  $pK$ -values and the  $\sigma_p^+$ -Hammett substituent constant [23], where;

$$pK = 0.40 - 1.42\sigma_p^+, \quad (r = 0.96) \quad (2)$$

According to this equation, electron-donating groups increase the charge density on the tertiary nitrogen atom of the benzoxazole ring due to the intramolecular CT interaction. Contrarily, the electron withdrawing groups reduce the charge density on the benzoxazole nitrogen atom. This is confirmed by the finding that the heterocyclic nitrogen atom of CN-SBO is protonated only in very strong acidic media ( $H_0$  from 0.33 to  $-1.17$ ) while that of  $Me_2N$ -SBO is protonated in buffers with pH-values in the range from 5.0 to 1.5.

The  $pK^*$ -values were also correlated with the substituent constant according to the equation;

$$pK^* = 2.29 - 4.55\sigma_p^+, \quad (r = 0.99) \quad (3)$$

The main result obtained from this correlation is the clear influence of the electronic properties of the substituents on protonation of the benzoxazole nitrogen. This effect is about three times more in the excited than in the ground state. The  $pK^*$ -values indicate also that the basicity of all styrylbenzoxazoles (except for CN-SBO) increases upon excitation. Further more, Table 5 shows that the magnitude of the basicity enhancement upon excitation depends strongly on the nature of the substituent. Unlike to the moderate enhancement of the basicity of Cl-SBO in the excited singlet state ( $\Delta pK = 1.56$ ), the basicity of  $Me_2N$ -SBO increases strongly upon excitation ( $\Delta pK = 7$  units). For CN-SBO, the situation is different where the excited state is less basic than the ground state ( $\Delta pK = -0.56$ ). This finding confirms strongly the previous discussion concerning the reversed direction of the ICT interaction in CN-SBO.

### 3.4. *Trans* $\rightarrow$ *cis* photoisomerization

In contrast to the lower  $\phi_f$ -values of all derivatives (except for CN-SBO), their *trans*  $\rightarrow$  *cis* photoisomerization at room temperature is efficient. Upon irradiation ( $\lambda_{irr} = 366$  or  $334$  nm) the absorbance at the absorption maximum decreases and eventually a photostationary state is approached. This is exemplified by Fig. 5, which displays the change in the absorption spectrum of  $CH_3O$ -SBO in ethanolic solution upon irradiation at  $365$  nm, as well as the growth of the *cis* isomer (%*cis*) with irradiation time. The composition of the photostationary state is displaced to the more *cis* isomer (contains from 65 to 88% *cis*, depending on the substituent and solvent) and its absorption maximum is relatively blue shifted. For CN-SBO, similar spectral changes were observed but the photostationary state is enriched in the *trans* isomer (contains from 39 to 60% *cis*). The *trans*  $\rightarrow$  *cis* photoisomerization reaction was studied in four solvents having different

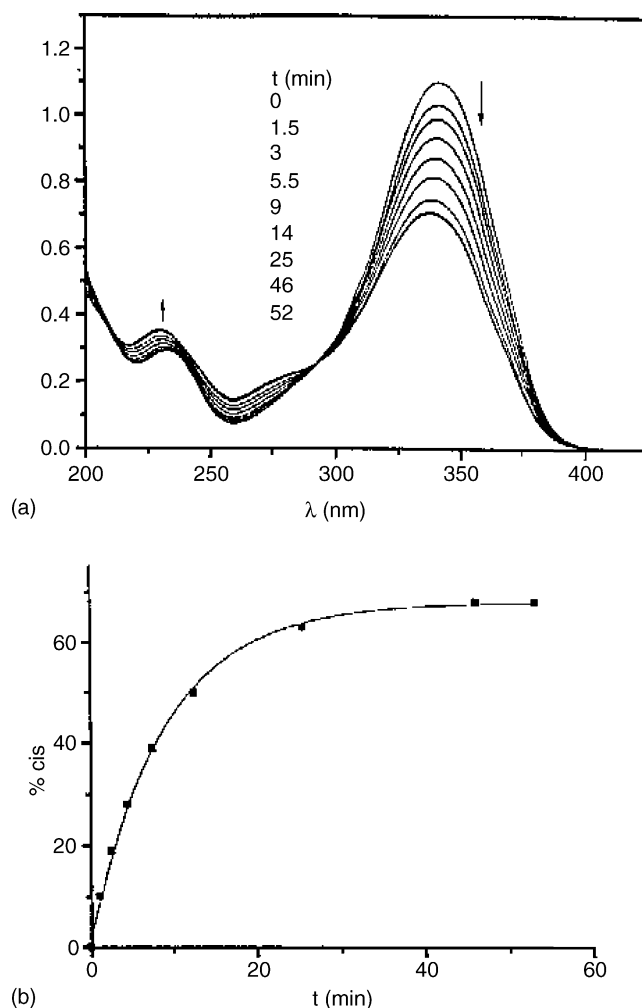


Fig. 5. (a) Change of the electronic absorption spectrum of  $CH_3O$ -SBO upon irradiation at  $365$  nm in ethanol. (b) Growth of the *cis* isomer (%*cis*) with the irradiation time for the same styryl dye in ethanol.

polarities and viscosities. The photoisomerization quantum yields ( $\phi_t$ ) were determined and reported in Table 6.

For  $-NMe_2$ ,  $2',4'$ - $OCH_3$ ,  $OCH_3$ ,  $CH_3$ ,  $H$  and  $Cl$ -derivatives, the  $\phi_t$  is substantial in all solvents except for Cl-SBO in *c*-hexane and H-SBO in ethylene glycol. Also, the  $\phi_t$ -values decrease on going from the non-viscous solvents as methanol to the more viscous solvents like ethylene glycol. However, this is not so for CN-SBO, which exhibits

Table 6  
*Trans*  $\rightarrow$  *cis* photoisomerization quantum yields ( $\phi_t$ ) of *R*-SBO in some solvents

<i>R</i>	<i>c</i> -Hexane	$CH_3CN$	MeOH	Et-glycol
$NMe_2$	0.10	0.13	0.16	0.077
$2',4'$ - $OCH_3$	0.15	0.21	0.19	0.11
$OCH_3$	0.20	0.17	0.15	0.12
$CH_3$	0.14	0.15	0.15	0.12
H	0.07	0.09	0.09	0.04
Cl	0.08	0.12	0.11	0.08
CN	0.02	0.04	0.07	0.04

the lowest  $\phi_t$ -values, where the photoisomerization quantum yield is less sensitive to the viscosity change. In contrast, its  $\phi_t$ -value decreases significantly in the non-polar solvents such as *c*-hexane. This trend is along the opposite direction of the polarity dependence of the fluorescence yield. Therefore, it was concluded that the radiative decay of the excited singlet state competes effectively with the photoisomerization process. This argument is further supported by studying the effects of substituents and solvent viscosity on both the fluorescence and photoisomerization quantum yields, which reveal that the two processes are complementary. As an evidence, is the enhancement of  $\phi_f$  in ethylene glycol on the expense of the radiationless *trans*  $\rightarrow$  *cis* photoisomerization. Additionally, CN-SBO exhibits the highest  $\phi_f$ -values and the lowest  $\phi_t$ -values in all solvents, compared to the other derivatives.

The dependence of the photoisomerization yields on the solvent polarity and viscosity suggest that the perpendicular state (phantom state responsible for the photoconversion) is reached from the ICT excited state. Also, the  $\phi_t$ -values for all derivatives are much smaller than the value reported for *trans*-stilbene ( $\phi_t \approx 0.5$ ) [36]. This indicates that the photoisomerization process is associated with higher torsional barriers for rotational motions around the central double bond. The reduced  $\phi_t$ -values in the viscous solvents as ethylene glycol, can be attributed to decreasing of the free-volume necessary for the twisting motions around the ethylenic double bond. This leads to increasing of the frictional forces and lowering of the isomerization yield.

Assuming that the decay of the perpendicular state yields a 1:1 ratio of *trans* and *cis* isomers [37], the sum of the fluorescence and photoisomerization quantum yields ( $\phi_f + 2\phi_t$ ) for CN-SBO in *c*-hexane, is within the experimental error close to 1.0 ( $\approx 0.89$ ). This suggests that other channels for non-radiative decay of the excited CN-SBO are of minor importance. For the other derivatives, the sum is much lower ( $< 0.5$ ) indicating that radiationless deactivation pathways, other than the photoreaction, are playing an important role in controlling the dynamics of the excited singlet state. Studying the photoisomerization of the present compounds seems to be of practical importance since applications of functional materials require both structural homogeneity and photostability.

## Acknowledgement

The authors would like to thank Prof. G. Grampp, TU-Graz, Austria, for providing the facility of fluorescence lifetime measurements.

## References

- [1] J. Saltiel, L.J. Charlton, *Rearrangements in Ground and Excited States*, Academic Press, New York, 1980.
- [2] D.H. Waldeck, *Chem. Rev.* 91 (1991) 415.
- [3] U. Mazzucato, *Pure Appl. Chem.* 54 (1982) 1705.
- [4] U. Mazzucato, F. Momicchioli, *Chem. Rev.* 91 (1991) 1679.
- [5] U. Mazzucato, G.G. Aloisi, F. Elisei, *Proc. Ind. Acad. Sci.* 105 (1993) 475.
- [6] R.V. Bensason, E.J. Land, T.G. Truscott, *Excited States and Free Radicals in Biology and Medicine*, Oxford University Press, New York, 1993.
- [7] G. Favaro, U. Mazzucato, F. Masetti, *J. Phys. Chem.* 77 (1973) 601.
- [8] G. Bartocci, U. Mazzucato, *Chem. Phys. Lett.* 47 (1977) 541.
- [9] L. Angeloni, E. Castelluci, G. Bartocci, U. Mazzucato, A. Spalletti, G. Marconi, *Gazz. Chem. Ital.* 126 (1996) 609.
- [10] L.C. Zhan, D.Y. Wang, *J. Photochem. Photobiol. A: Chem.* 147 (2002) 93.
- [11] M.M. Muir, O. Cox, L.A. Rivera, M.E. Cadiz, E. Medina, *Inorg. Chim. Acta* 191 (1992) 131.
- [12] C.M. Lazano, O. Cox, M. Muir, J.D. Morales, J.L. Rodrigues-Caban, P.E. Vivas-Mejia, F.A. Gonzales, *Inorg. Chim. Acta* 271 (1998) 137.
- [13] B. Jeffery, P. Sanfilippo, *Applications US*, 87 (1987).
- [14] K. Suzuki, *Applications Jp*, 87 (1987).
- [15] A.M. Weaver, P.W. Pruett, D.S. Hilbert, D.R. Burpitt, *Applications US*, 10 (1989).
- [16] K. Ting, W.Y. Mei, M.J. Ben, *Chin. Chem. Lett.* 7 (1996) 641.
- [17] V. Tralic-Kulenovic, L. Fiser-Jakic, *Spectrochim. Acta* 53A (1997) 271.
- [18] T.A. Fayed, S.H. Etaiw, *Mont. Chem.* 130 (1999) 1319.
- [19] T.A. Fayed, *J. Photochem. Photobiol. A: Chem.* 121 (1999) 17.
- [20] M. Ikegami, T. Akai, *J. Chem. Soc. Perkin Trans. 2* (2002) 342.
- [21] T.A. Fayed, *Colloids Surf. A: Physicochem. Eng. Aspects* 236 (2004) 171.
- [22] C.H. Rochester, *Acidity Functions*, Academic Press, London, New York, 1970.
- [23] S.L. Murov, I. Carmichael, G.L. Hug, *Handbook of Photochemistry*, 2nd edn., Marcel Dekker, New York, 1993.
- [24] J.V. Morris, M.A. Mahaney, I.R. Huber, *J. Phys. Chem.* 80 (1976) 971.
- [25] G. Gauglitz, *J. Photochem.* 5 (1976) 41.
- [26] S. Landgraf, *Spectrochim. Acta* 57A (2001) 2029.
- [27] I.A.Z. Al-Ansari, *J. Phys. Org. Chem.* 10 (1997) 687.
- [28] P. Bosch, A. Fernandez-Arizpe, J.L. Mateo, A.E. Lozano, P. Noheda, *J. Photochem. Photobiol. A: Chem.* 133 (2000) 51.
- [29] F. Würthner, R. Sens, K.H. Etzbach, G. Seybold, *Angew. Chem. Int.* 38 (1999) 1649.
- [30] S.A. Jenekhe, *Adv. Mater.* 7 (1995) 309.
- [31] D.Y. Kim, H.N. Cho, C.Y. Kim, *Prog. Polym. Sci.* 25 (2000) 1089.
- [32] E.M. Kosower, R. Giniger, A. Radkowsky, D. Hebel, A. Shusterman, *J. Phys. Chem.* 90 (1986) 5552.
- [33] H.S. Joshi, R. Jamshidi, Y. Tor, *Angew. Chem. Int.* 38 (1999) 2722.
- [34] A.W. Czarnik, *Fluorescent Chemosensors for Ion and Molecule Recognition*, American Chemical Society, Washington, DC, 1992.
- [35] E. Fortster, *Z. Elektrochem.* 54 (1950) 531.
- [36] F.D. Lewis, R.S. Kalgutkar, J.S. Yang, *J. Am. Chem. Soc.* 121 (1999) 12045.
- [37] J. Saltiel, A.S. Waller, D.F. Sears, E.A. Hoburg, D.M. Zeglinski, D.H. Waldeck, *J. Phys. Chem.* 98 (1994) 10689.